Materials Physics and Mechanics 47 (2021) 665-675
Research article

Received: September 7, 2021
Accepted: October 12, 2021

POST-DYNAMIC RECRYSTALLIZATION IN A HEAVILY ALLOYED NI-BASED SUPERALLOY

Artem Ganeev✉, Rishat Zainullin, Ruslan Shakhov, Shamil Mukhtarov, Valery Imayev

Institute for Metals Superplasticity Problems of RAS. 39 Khalturin St., Ufa, 450001, Russia

✉ artem@imsp.ru

Abstract. The work is devoted to a study of post-dynamic recrystallization in a recently developed nickel-based superalloy SDZhS-15 manufactured by ingot metallurgy and intended for disc applications. The as-cast superalloy was subjected to long-term homogenization annealing and canned forging at subsolvus temperatures (T=Ts-(40-70), where Ts is the γ′ solvus temperature) under quasi-isothermal conditions. This led to the formation of a refined recrystallized fine-grained structure with individual non-recrystallized γ grains in the central part of the forged workpiece. However, in the near-surface layers of the forged workpiece, the volume fraction of non-recrystallized grains was appreciably higher. To further recrystallize the as-forged microstructure the recrystallization annealing was performed at a temperature (T=Ts-70) for different times to obtain a homogeneous recrystallized and fine-grained structure (d_γ<10 μm) without causing a strong grain growth. The produced microstructures were examined by scanning electron microscopy including the electron backscattered diffraction technique. It was established that the increase of the annealing time led to the refinement of coarse non-recrystallized γ grains and insignificant coarsening of fine-grained recrystallized structure. The fraction of high-angle grain/interphase boundaries including twin boundaries increased. It was revealed that the use of the recrystallization annealing resulted in a slower γ grain growth during subsequent solid solution treatment in contrast to the conditions obtained via forging followed by solid solution treatment. Based on the performed work, the processing route of the heavily alloyed ingot-metallurgy SDZhS-15 superalloy was specified. It should include homogenization annealing, canned hot forging at subsolvus temperatures, post-forging recrystallization annealing, solid solution treatment, and ageing.
Keywords: nickel-based superalloy, microstructure, recrystallization annealing, solid solution treatment, grain/interphase boundaries

Acknowledgements. *The present work was supported by the Ministry of Science and Higher Education of the Russian Federation in accordance with the State Assignment of the Institute for Metals Superplasticity Problems of Russian Academy of Sciences (AAAA-A17-117041310215-4). The work was performed using the facilities of the shared services center «Structural and Physical-Mechanical Studies of Materials» at the Institute for Metals Superplasticity Problems of Russian Academy of Sciences.*

Citation: Ganeev Artem, Zainullin Rishat, Shakhov Ruslan, Mukhtarov Shamil, Imayev Valery. Post-dynamic recrystallization in a heavily alloyed Ni-based superalloy // Materials Physics and Mechanics. 2021, V. 47. N. 5. P. 665-675. DOI: 10.18149/MPM.4752021_1.

http://dx.doi.org/10.18149/MPM.4752021_1

1. Introduction

Polycrystalline nickel-based superalloys are widely used as structural materials in gas turbine engines (GTE), particularly as disc materials. The discs are critical GTE parts for which it is important to carefully control the microstructure and, in particular, the γ grain size because of its strong influence on the mechanical properties of the produced discs [1-4]. The key challenge for controlling the γ grain size and attaining enhanced mechanical properties is to achieve a homogeneous fine-grained structure ($d_\gamma \leq 10$ мкм) [3,5-8]. However, the achievement of a fully recrystallized and fine-grained structure in discs made of heavily alloyed nickel-based superalloys is a complex technical task especially in the case of the ingot-metallurgy material. Firstly, the nickel-based disc superalloys possess limited deformability [9]. Secondly, any wrought processing can not provide a uniform development of dynamic recrystallization in the wrought product (first of all because of friction forces arising between the workpiece and the die tool and leading to the inhomogeneous occurrence of the deformation throughout the workpiece) [10,11,12]. Thirdly, recrystallization annealing and/or solid solution treatment of the hot worked material near the γ′ solvus temperature promotes recrystallization processes but often leads to undesirable γ grain growth [13-17]. To increase the homogeneity of the hot worked material, it makes sense to perform post-dynamic recrystallization annealing in order to hinder fast γ grain growth [18].

The present work was aimed to study the influence of recrystallization annealing and subsequent solid solution treatment on the microstructure of the hot-forged workpiece of the SDZhS-15 superalloy. In our previous works [3,19,20], the processing route containing homogenization heat treatment, canned forging, solid solution treatment, and ageing was developed for this superalloy. However, canned forging did not provide the formation of a homogeneous recrystallized microstructure throughout the workpiece volume. In the present work, particular attention was paid to the near-surface layers of the forged workpiece, in which the volume fraction of coarse non-recrystallized γ grains was rather high. The microstructure obtained after forging, recrystallization annealing, and solid solution treatment is compared with that obtained after forging and solid solution treatment.

The SDZhS-15 superalloy was developed as a disc material with operating temperatures up to 850°C. As was earlier shown [3,19,20], this superalloy demonstrated high mechanical properties as compared with currently known disc superalloys. Nevertheless, further investigations are required to improve the microstructure control and to reach enhanced mechanical properties.

2. Materials and experimental

The SDZhS-15 superalloy with a nominal chemical composition of (Ni-28(Cr,Co)-12.5(Al,Ti,Nb,Ta)-9(Mo,W,Re)-0.17(C,La,Y,Ce,B), wt.%) was manufactured by vacuum induction melting as an ingot with a diameter of 140 mm. The γ′ (Ni_3Al) solvus temperature was earlier determined as T_s=1220±5°C by quenching experiments [19,20]. The as-cast material was subjected to long-term homogenization annealing at near the γ′ solvus temperature followed by slow cooling with a rate of 25°C/h, which was applied to obtain possibly coarse γ′ particles and thus to improve the hot workability [19,20]. The cylinders with a size of Ø37 mm×50 mm were cut from the homogenized material for subsequent forging. The cylinders were encapsulated in stainless steel cans, which protected from fast cooling and promoted quasi-hydrostatic pressure during forging, somewhat reducing the negative influence of friction forces arising between the forged workpiece and the die tool. The forging was performed under quasi-isothermal conditions in two stages with intermediate annealing at subsolvus temperatures, followed by air cooling as described elsewhere [19,20]. Using such a technique, sound forgings with an approximate size of Ø75×12 mm were obtained.

The obtained forgings were cut into pieces. Some of them were subjected to recrystallization annealing at 1150°C during 1, 2, 4, 8, and 16 h, and some of them were subjected to solid solution treatment at 1160, 1170, 1180, 1190, and 1200°C during 1 h followed by air cooling. The solution treatments were also performed for the materials subjected to recrystallization annealing at 1150°C (8 h).

Microstructure examination of the forged and heat-treated workpieces was performed approximately for the central cross-section taking into consideration the central area (zone 1) and the peripheral area (zone 2) at the distance of about 2.5 mm from the flat surface of the forged workpiece as shown in Fig. 1. Scanning electron microscopy was used for microstructure examination. The electron backscatter diffraction (EBSD) analysis was performed on 450×450 μm^2 area with a scan-step size of 0.5 μm using the HKL Channel 5 software. The grain/interphase boundaries having a misorientation angle less than 2° were excluded from the data analysis taking into account the measurement accuracy. The grain boundaries having a misorientation angle of more than 15° were assumed as high-angle ones. After EBSD measurements the same areas were taken for BSE images, which were used for separating the γ grains and coarse primary γ′ particles. The sizes of γ grains and γ′ precipitates were measured using the intercept method. For quantifying the twin boundaries the length of twin boundaries (L_{TB}) per unit area (L_A) was calculated by the following equation: $L_A=L_{TB}/A$, where L_{TB} is the total length of the twin boundaries defined for area A. To determine the length of the twin boundaries (L_{TB}) the map corresponding to Σ3 boundaries with a size of 900×900 pixels was obtained and the calculated number of pixels falling on these boundaries was multiplied by the scan-step size (0.5 μm). The development of recrystallization after recrystallization annealing was assessed taking into account the fraction of high-angle grain/interphase boundaries and the kernel average misorientation (KAM) maps. The γ grains were considered non-recrystallized if they contained many low-angle boundaries and areas of local misorientations shown by the KAM maps.

3. Results and discussion

Microstructure examination of the forged workpiece. Figure 1 represents the macrostructure obtained from the central cross-section of the forged workpiece and Fig. 2 shows the microstructures obtained in zones 1 and 2. In zone 1, near fully recrystallized microstructure with predominantly high-angle grain/interphase boundaries was formed. The mean γ grain size was d_γ=4.3±0.3 μm, the mean size of the secondary γ′ phase, which precipitated after forging during air cooling was $d_{\gamma'}$=0.25±0.03 μm. The primary γ′ phase was located mostly along γ grain boundaries, its mean size was $d_{\gamma'}$=3.6±0.3 μm. The volume fraction of the non-recrystallized structure did not exceed 10%. In the interior of the non-recrystallized γ grains the mean size of the secondary γ′ phase was the same, $d_{\gamma'}$=0.25±0.03 μm, the mean size of the primary γ′ phase was $d_{\gamma'}$=2±0.2. In zone 2, the volume fraction of recrystallized structure was only about 40%. Non-recrystallized γ grains had a size of 50-100 μm and contained many low-angle boundaries. The mean sizes of the recrystallized γ grains and the γ′ precipitates in zone 2 were near the same as in zone 1.

Thus, the friction forces arising between the die tool and the forged workpiece during forging led to the inhomogeneous occurrence of recrystallization processes throughout the forged workpiece. Recrystallization annealing was performed to recrystallize the microstructure first of all in the near-surface layers of the forged workpiece. This annealing was carried out in order to avoid fast γ grain growth.

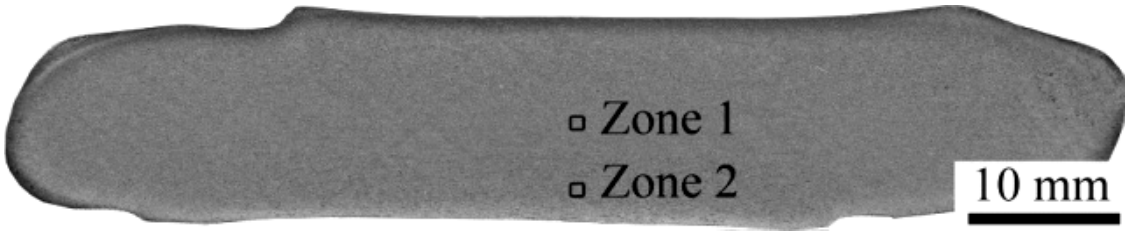

Fig. 1. The macrostructure of the SDZhS-15 superalloy forging central cross-section. The microstructure analysis was performed from zones 1 and 2

Effect of recrystallization annealing on the microstructure of the forged workpiece. Figure 3 shows the EBSD orientation maps and the KAM maps obtained from zone 2 after forging and recrystallization annealing at 1150°C during 1-16 hours. Figure 4 represents the influence of recrystallization annealing at 1150°C on the microstructure parameters. Comparing Figs. 2b and 3 one can see that recrystallization annealing leads to the graduate disappearance of coarse non-recrystallized γ grains.

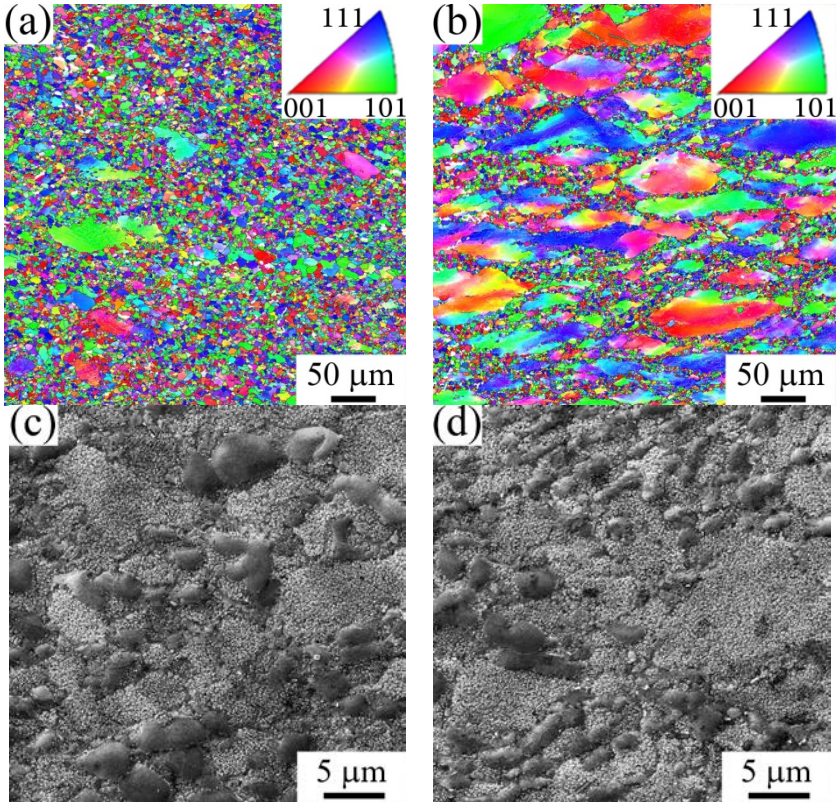

Fig. 2. (a,b) EBSD orientation maps (normal-direction inverse pole figures) and (c,d) BSE images obtained from the central cross-section of the forged workpiece: (a and c) zone 1, (b and d) zone 2

This is accompanied by the increase of the fraction of high-angle grain/interphase boundaries and the length of twin boundaries per unit area, suggesting that non-recrystallized γ grains were gradually recrystallized during annealing at 1150°C (Fig. 4a,b). For instance, the fraction of high-angle boundaries in zone 2 increased from 48 to 87% after annealing during 8 and 16 hours. The length of twin boundaries per unit area in zones 1 and 2 increased from 50 to 145-157 mm^{-1} after 16 hours. The KAM maps show that non-recrystallized γ grains after annealing during 8 and 16 hours were not detected. It is worth noting that recrystallization was not accompanied by the significant growth of fine recrystallized γ grains.

After annealing during 8 and 16 hours the mean γ grain size increased from d_γ=4.3 μm to d_γ=6.7 and 7.2 μm, respectively (Fig. 4c).

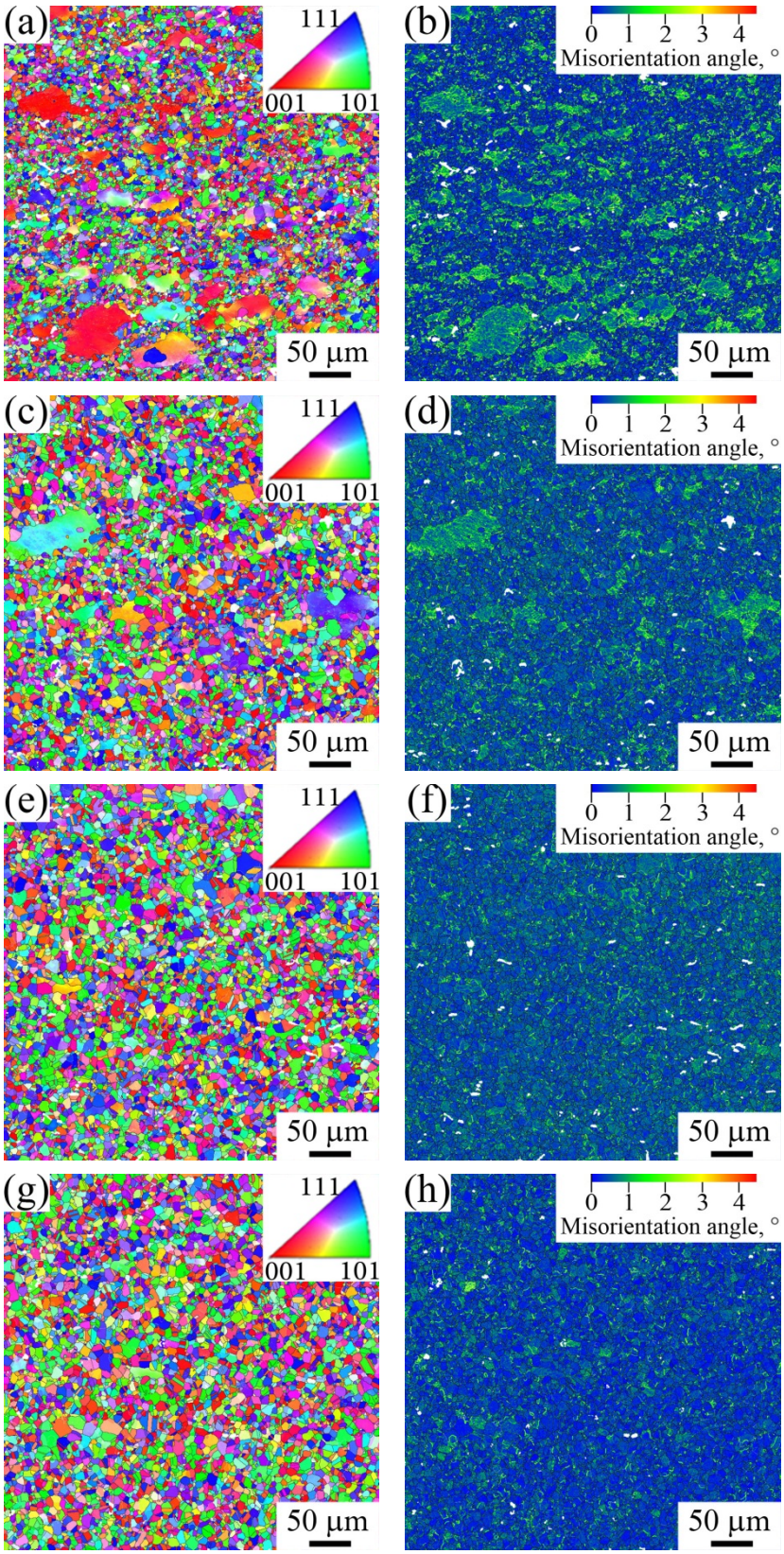

Fig. 3. (a,c,e,g) EBSD orientation maps (normal-direction inverse pole figures) and (b,d,f,h) KAM maps (c,d) obtained from zone 2 after forging and recrystallization annealing at 1150°C during 1-16 h: (a,b) 1 h, (c,d) 4 h, (e,f) 8 h, (g,h) 16 h

Thus, non-recrystallized areas in the near-surface layers of the forged workpieces of the SDZhS-15 superalloy can be successfully recrystallized using recrystallization annealing without causing a strong grain growth. Recrystallization annealing led to the increase of the fraction of high-angle boundaries including twin boundaries. Note that the twin boundaries are favorable for increasing the creep and crack growth resistance [21]. Based on the quantitative estimates, recrystallization annealing at 1150°C for 8 hours was chosen as the optimal.

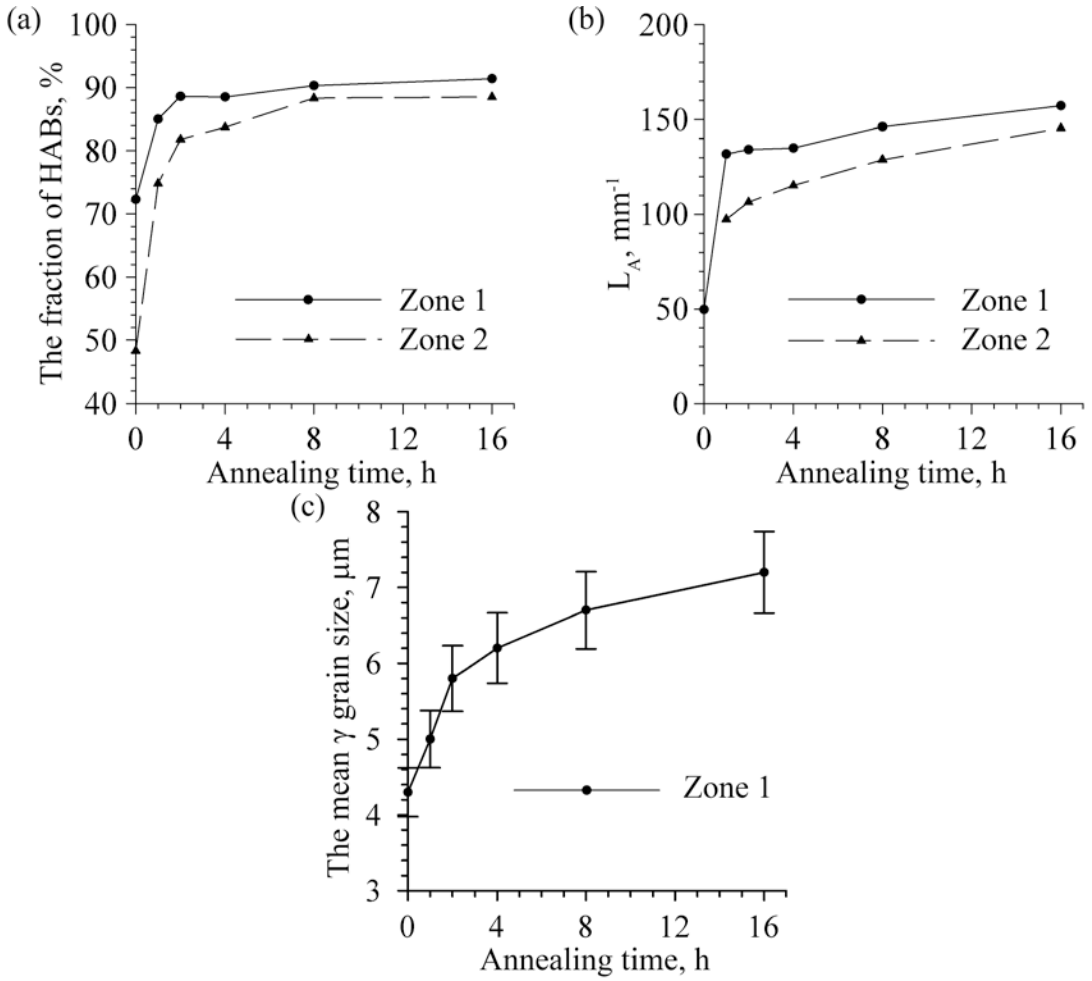

Fig. 4. Effect of recrystallization annealing at 1150°C on (a) the fraction of high-angle grain/interphase boundaries (HABs), (b) the length of twin boundaries per unit area (L_a) in zones 1 and 2 and (c) the γ grain growth in zone 1

Effect of solid solution treatment on the microstructure obtained after forging and recrystallization annealing. As was shown in our previous work [3], solid solution treatment followed by ageing is required to attain enhanced mechanical properties in the SDZhS-15 superalloy. However, the solution treatment can be carried out both immediately after forging and after forging with the following recrystallization annealing. Figure 5 shows the effect of the solution treatment temperature on (a) the fraction of high-angle grain/interphase boundaries, (b) the length of twin boundaries per unit area, and (c) the γ grain size in zone 1 of the forged workpiece. An increase in the solution treatment temperature led to insignificant changes in the fraction of the high-angle boundaries, which was slightly higher in the case of the processing route including recrystallization annealing. With increasing the solution treatment temperature the length of twin boundaries per unit area decreased and the γ grain size increased. It is worth noting that the length of twin boundaries was always higher and the

γ grain size was appreciably smaller after solution treatment at T>1160°C in the case of the processing route including recrystallization annealing. Particularly, the mean γ grain size after solution treatment at 1180°C is d_γ= 9.3±0.7 μm after processing route including recrystallization annealing and d_γ= 14.2±1 μm without recrystallization annealing (Figs. 5c and 6). Slower grain growth in the first case should be ascribed to the higher volume fraction of fine recrystallized γ grains with a low dislocation density before solution treatment and, therefore, a thermodynamic driving force for grain growth in the first case was smaller than that in the case of the processing route without recrystallization annealing. A smaller γ grain size and a higher length of twin boundaries per unit area in the case of the processing route including recrystallization annealing should be favorable for mechanical properties. Therefore, the processing route of a heavily alloyed nickel-base superalloy produced by ingot-metallurgy should include recrystallization annealing between hot forging and solid solution heat treatment.

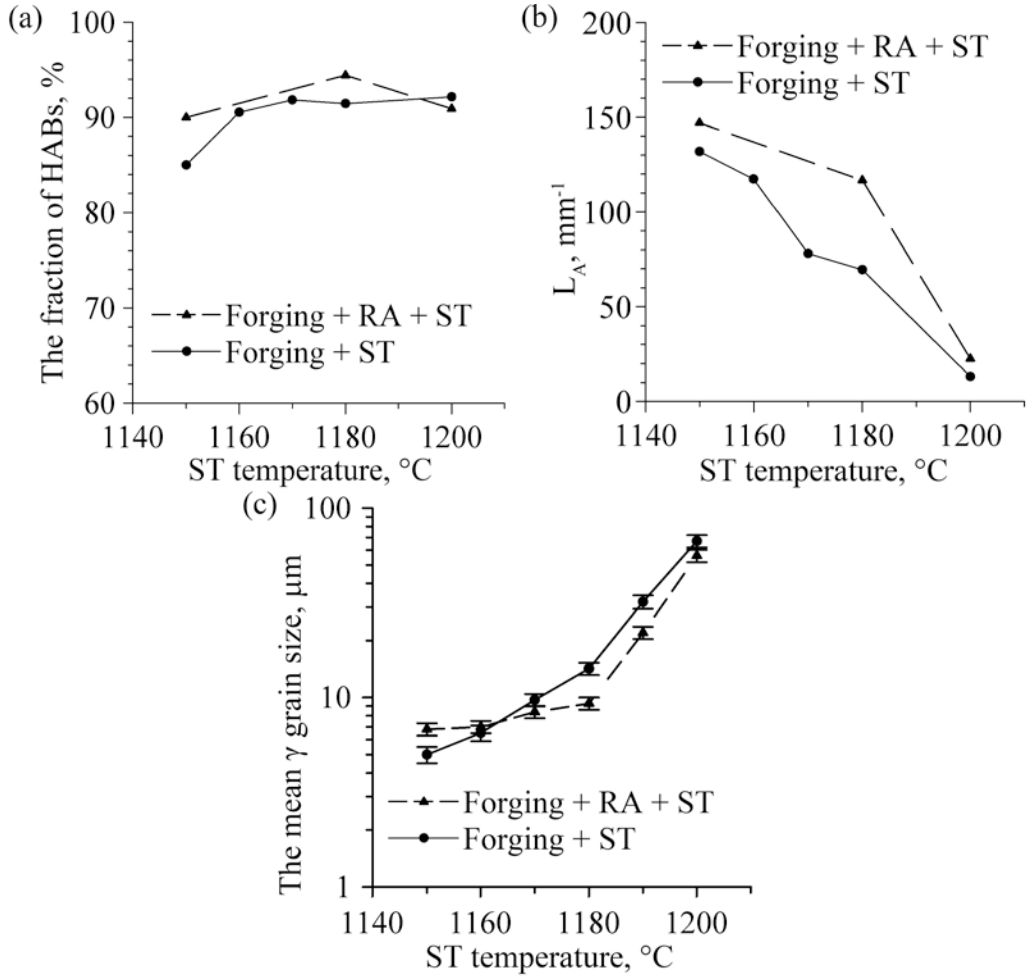

Fig. 5. Effect of the solution treatment (ST) temperature on (a) the fraction of high-angle grain/interphase boundaries (HABs), (b) the length of twin boundaries per unit area (L_a), and (c) the γ grain growth in zone 1. The solution treatment was performed after forging, recrystallization annealing (RA) at 1150°C (8 h), and after forging only

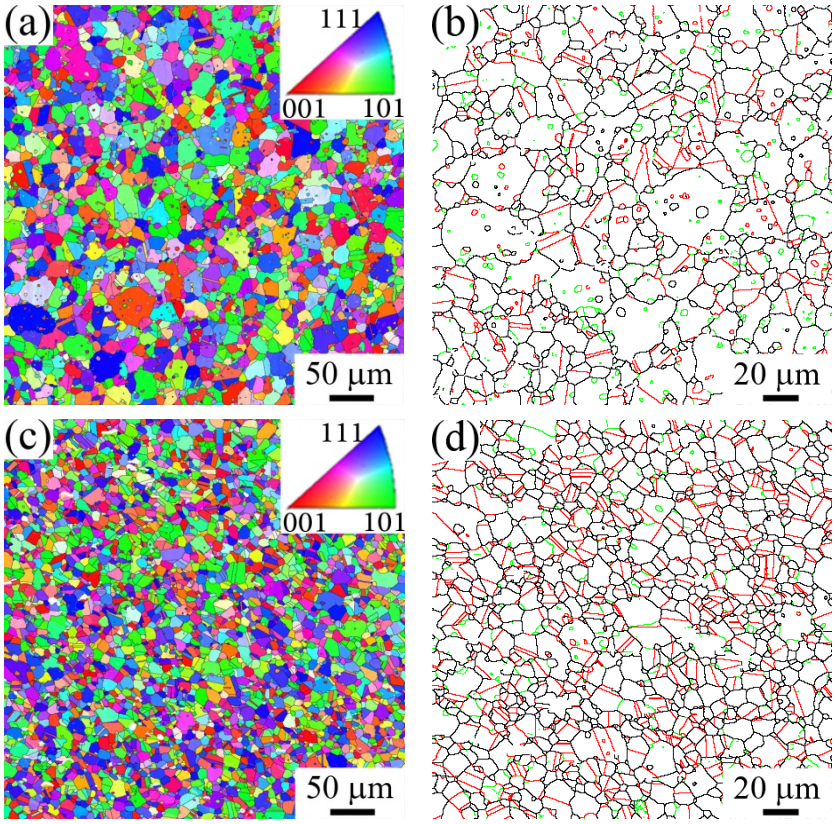

Fig. 6. (a,c) EBSD orientation maps (normal-direction inverse pole figures) and (b,d) grain boundaries network highlighting the random high angle boundaries (black), Σ3 twin boundaries (red), and low angle boundaries (green) obtained for zone 1 (a,b) after forging and solution treatment and (c,d) after forging, recrystallization annealing and solution treatment. The solution treatment was performed at 1180°C

Table 1. Processing route proposed for heavily alloyed disc nickel-based superalloys produced by ingot-metallurgy

Processing stage	The aims of the processing stage
Homogenization treatment at neat the γ′ solvus temperature	- An increase of the chemical homogeneity, dissolution of dendritic segregations; - coarsening of the γ′ phase and, as a result, an increase of the hot workability.
Canned two- or three-stage hot forging with intermediate annealing at subsolvus (T_s-(40-70)) temperatures	- Refinement of the as-cast microstructure via recrystallization processes; - an increase of the dislocation density in poorly recrystallized near-surface layers of the workpiece (large γ grains).
Recrystallization annealing at temperature (T_s-70)	- An increase of the volume fraction of recrystallized microstructure up to almost 100%, while retaining a fine-grained structure ($d_\gamma \leq 10$ μm)
Solid solution treatment at subsolvus temperatures (T_s-(40-50))	- Precipitation of the secondary γ′ phase as particles with a size of about 0.1 μm
Ageing	- Precipitation of the tertiary γ′ phase as particles with a size of less than 0.1 μm

Table 1 schematically describes the processing route proposed for heavily alloyed disc nickel-based superalloys produced by ingot-metallurgy and the aims of each processing stage, which should be attained for enhanced mechanical properties.

The presented results show that the processing route for the SDZhS-15 superalloy should be specified. Hot forging should be followed by recrystallization annealing and only then solution treatment and ageing. The use of intermediate recrystallization annealing allowed us to near completely recrystallize the forged material that in its turn provided smaller γ grain size and higher length of twin boundaries after solution heat treatment at subsolvus temperatures. As expected, this should be favorable for attaining enhanced mechanical properties.

4. Conclusions

The influence of post-forging recrystallization annealing and solid solution treatment on the microstructure of the forged workpiece was investigated for the heavily alloyed nickel-based superalloy SDZhS-15 produced by ingot-metallurgy. The following main conclusions can be drawn:

- recrystallization annealing at $T=T_s$-70 after canned forging at $T=T_s$-(40-70) led to the effective development of recrystallization processes in the near-surface layers of the forged workpiece, in which the volume fraction of coarse non-recrystallized γ grains after forging was rather high. The optimal recrystallization annealing was at 1150°C (8 h);

- recrystallization annealing at 1150°C (8 h) led to the disappearance of non-recrystallized γ grains, the increase of the fraction of high-angle grain/interphase boundaries including twin boundaries while retaining a fine-grained structure ($d_\gamma \leq 10$ μm);

- post-forging recrystallization annealing slowed down grain growth during solid solution treatment;

- the obtained results allowed us to specify the processing route for the SDZhS-15 superalloy. Canned hot forging should be followed by recrystallization annealing and only then solution treatment and ageing. As expected, this should be favorable for attaining enhanced mechanical properties.

References

[1] Reed RC. *The Superalloys: Fundamentals and Applications.* Cambridge: Cambridge University Press; 2006.

[2] Pollock TM, Tin S. Nickel-Based Superalloys for Advanced Turbine Engines: Chemistry, Microstructure, and Properties. *Journal of propulsion and power*. 2006;22(2): 361-374.

[3] Imayev V, Mukhtarov S, Mukhtarova K, Ganeev A, Shakhov R, Parkhimovich N, Logunov A. Influence of forging and heat treatment on the microstructure and mechanical properties of a heavily alloyed ingot-metallurgy nickel-based superalloy. *Metals.* 2020;10(12): 1606.

[4] Thébaud L, Villechaise P, Crozet C, Devaux A, Béchet D, Franchet J-M, Rouié A-L, Mills M, Cormier J. Is there an optimal grain size for creep resistance in Ni-based disk superalloys? *Materials Science & Engineering A.* 2018;A716: 274-283.

[5] Xiong Y, Yang A, Guo Y, Liu W, Liu L. Effect of fine-grained structure on the mechanical properties of superalloys K3 and K4169. *Science and Technology of Advance Materials.* 2001;2(1): 7-11.

[6] Lee H, Hou W. Fine grains forming process, mechanism of fine grain formation and properties of superalloy 718. *Materials Transactions.* 2012;53(4): 716-723.

[7] Lee H, Hou W. Development of fine-grained structure and the mechanical properties of nickel-based Superalloy 718. *Materials Science and Engineering A.* 2012;555: 13-20.

[8] Gayda J, Kantzos P. *Burst testing of a superalloy disk with a dual grain structure.* National Aeronautics and Space Administration; 2002.
[9] Locq D, Caron P. On some advanced nickel-based superalloys for disk applications. *Aerospace Lab, Alain Appriou*. 2011;3: 1-9.
[10] He G, Tan L, Liu F, Huang L, Huang Z, Jiang L. Unraveling the formation mechanism of abnormally large grains in an advanced polycrystalline nickel base superalloy. *Journal of Alloys and Compounds.* 2017;718: 405-413.
[11] Ganeev AA, Valitov VA, Akhunova AK, Utyashev FZ. Influence of the container design on the stress-strain state of a billet made of hard-to-deform granular EP741NP alloy. In: *Proc. XII Congress of Mechanics in Ufa*. 2019. p.290-292. (In Russian)
[12] Kañetas PJP, Calvo J, Rodriguez-Calvillo P, Cabrera Marrero JM, Zamora Antuñano MA, Guerrero-Mata MP. EBSD Study of Delta-Processed Ni-Based Superalloy. *Metals.* 2020;10(11): 1466.
[13] Nicolaÿ A, Fiorucci G, Franchet JM, Cormier J, Bozzolo N. Influence of strain rate on subsolvus dynamic and post-dynamic recrystallization kinetics of Inconel 718. *ActaMaterialia.* 2019;174: 406-417.
[14] McCarley J, Tin S. Utilization of hot deformation to trigger strain induced boundary migration (SIBM) in Ni-base superalloys. *Materials Science & Engineering A.* 2018;720: 189-202.
[15] Poelt P, Sommitsch C, Mitsche S, Walter M. Dynamic recrystallization of Ni-base alloys - Experimental results and comparisons with simulations. *Materials Science & Engineering A.* 2006;420: 306-314.
[16] Eriksson E, Colliander MH. Dynamic and Post-Dynamic Recrystallization of Haynes 282 below the Secondary Carbide Solvus. *Metals.* 2021;11(1): 122.
[17] Wang GQ, Chen MS, Lin YC, Li HB, Zeng WD, Ma YY, Cai JL, Peng CX, Zou FY. A novel annealing method to uniformly refine deformed mixed grain microstructure of a solution-treated Ni-based superalloy. *Sci China Tech Sci*. 2021;64: 1741-1751.
[18] Sakai T, Belyakov A, Kaibyshev R, Miura H, Jonas John J. Dynamic and post-dynamic recrystallization under hot, cold and severe plastic deformation conditions. *Progress in Materials Science.* 2014;60: 130.
[19] Mukhtarov SK, Imayev VM, Logunov AV, Shmotin YN, Mikhailov AM, Gaisin RA, Shakhov RV, Ganeev AA, Imayev RM. Recrystallisation behaviour and mechanical properties of a novel Re-containing nickel-base superalloy. *Mater. Sci. Technol.* 2019;35(13): 1605-1613.
[20] Imayev VM, Mukhtarov SK, Logunov AV, Ganeev AA, Shakhov RV, Imayev RM. Effect of thermomechanical treatment on the microstructure and mechanical properties of a novel heavily alloyed nickel base superalloy. *Letters on Materials.* 2019;9(2): 249-254.
[21] Bozzolo N, Bernacki M. Viewpoint on the Formation and Evolution of Annealing Twins During Thermomechanical Processing of FCC Metals and Alloys. *Metallurgical and materials transactions A.* 2020;51A: 2665-2684.

THE AUTHORS

Ganeev A.A.
e-mail: artem@imsp.ru
ORCID: 0000-0002-2680-4256

Zainullin R. I.
e-mail: zayn.rishat@yandex.ru
ORCID: 0000-0002-2418-8218

Shakhov R. V.
e-mail: shakhov@imsp.ru
ORCID: 0000-0001-8669-5293

Mukhtarov Sh. Kh.
e-mail: shamil@anrb.ru
ORCID: 0000-0003-0756-4418

Imayev V. M.
e-mail: vimayev@mail.ru
ORCID: 0000-0002-0060-5478